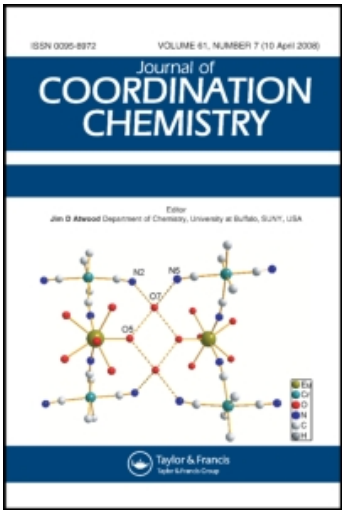

Journal of Coordination Chemistry

Publication details, including instructions for authors and subscription information:
http://www.informaworld.com/smpp/title~content=t713455674

Synthesis and structural characterization of nitrite-coordinating Co^{II} and Co^{III} complexes as models for the reaction center of Co-substituted nitrite reductase

Hiroshi Yokoyama[ab]; Aya Masuno[a]; Makoto Misoo[a]; Kazuya Yamaguchi[a]; Shinnichiro Suzuki[a]
[a] Department of Chemistry, Graduate School of Science, Osaka University, Toyonaka 560-0043, Osaka, Japan [b] Bio-Industry Division, Manufacturing Industries Bureau, Ministry of Economy, Trade and Industry, Chiyoda-ku, Tokyo 100-8901, Japan

Online publication date: 08 March 2010

To cite this Article Yokoyama, Hiroshi , Masuno, Aya , Misoo, Makoto , Yamaguchi, Kazuya and Suzuki, Shinnichiro(2010) 'Synthesis and structural characterization of nitrite-coordinating Co^{II} and Co^{III} complexes as models for the reaction center of Co-substituted nitrite reductase', Journal of Coordination Chemistry, 63: 5, 762 — 775
To link to this Article: DOI: 10.1080/00958971003674417
URL: http://dx.doi.org/10.1080/00958971003674417

Journal of Coordination Chemistry
Vol. 63, No. 5, 10 March 2010, 762–775

Synthesis and structural characterization of nitrite-coordinating Co^{II} and Co^{III} complexes as models for the reaction center of Co-substituted nitrite reductase

HIROSHI YOKOYAMA†‡, AYA MASUNO†, MAKOTO MISOO†, KAZUYA YAMAGUCHI† and SHINNICHIRO SUZUKI*†

†Department of Chemistry, Graduate School of Science, Osaka University, Toyonaka 560-0043, Osaka, Japan
‡Bio-Industry Division, Manufacturing Industries Bureau, Ministry of Economy, Trade and Industry, 1-3-1 Kasumigaseki, Chiyoda-ku, Tokyo 100-8901, Japan

(*Received 22 July 2009; in final form 29 October 2009*)

Co^{II} and Co^{III} complexes containing nitrite and tridentate aromatic amine compounds [bis(6-methyl-2-pyridylmethyl)amine (Me_2bpa) and bis(2-pyridylmethyl)amine (bpa)] have been prepared as models of the catalytic center in Co-substituted nitrite reductase: $[Co^{II}(Me_2bpa)(NO_2)Cl]_2 \cdot$acetone (**2**), $Co^{II}(Me_2bpa)(NO_2)_2$ (**3**), $Co^{II}(bpa)(NO_2)Cl$ (**4**), $Co^{II}(bpa)(NO_2)_2$ (**5**), $Co^{III}(Me_2bpa)(NO_2)(CO_3)$ (**6**), and $Co^{III}(bpa)(NO_2)_3$ (**7**). The X-ray crystal structure analyses of these Co^{II} and Co^{III} complexes indicated that the geometries of the cobalt centers are distorted octahedral and the Me_2bpa and bpa with three nitrogen donors exhibit *mer*- (**2**, **3**, and **7**) and *fac*-form (**4** and **6**). The coordination mode of nitrite depends on the cobalt oxidation state, to Co^{II} through the oxygen (nitrito coordination, *O*- and *O*,*O*-coordination) and to Co^{III} through nitrogen (nitro coordination, *N*-coordination mode). These findings are consistent with the results of their IR spectra, except that another oxygen of the *O*-coordinated nitrito group in **3** might interact weakly with Co^{II} according to its IR spectrum. Reductions of the nitrite in **2**, **3**, **4**, and **5** to nitrogen monoxide were not accelerated in the presence of proton, perhaps due to the nitrito coordination in these Co^{II} complexes.

Keywords: Co^{II} complexes; Co^{III} complexes; Nitrite complexes; Nitrite reductase

1. Introduction

Nitrite reductase, a key enzyme of denitrification, catalyzes the one-electron reduction of nitrite to nitrogen monooxide ($NO_2^- + 2H^+ \rightarrow NO + H_2O$). Cu-containing nitrite reductase (Cu-NIR) is a 110 kDa homotrimer, in which a monomer contains one type 1 Cu (electron transfer center) and one type 2 Cu (reaction center) [1, 2]. The X-ray crystal structures of trimeric Cu-NIRs [3–6] demonstrate that the interatomic distance between these Cu sites bound by the Cys-His sequence segment is *ca* 12.5 Å. The type 1 Cu having 2His, Cys, Met is located in a monomer, while the type 2 Cu site having three His ligands and one water is ligated at the interface formed by two adjacent monomers.

*Corresponding author. Email: bic@ch.wani.osaka-u.ac.jp

ISSN 0095-8972 print/ISSN 1029-0389 online © 2010 Taylor & Francis
DOI: 10.1080/00958971003674417

The structures of nitrite-soaked oxidized Cu-NIRs demonstrated that the substrate is coordinated to the type 2 Cu^{II} in an asymmetric bidentate fashion through two oxygens instead of the water [4, 5, 7].

Co^{II}-substituted NIRs (Co^{II}NIRs) from *Achromobacter cycloclastes* and *Achromobacter xylosoxidans* have been reported [8, 9]. Cobalt(II) is generally suitable as an environmental probe because of the high sensitivity of its visible absorption and magnetic circular dichroism spectra for d–d transitions [10]. The electronic absorption and magnetic circular dichroism spectra of the Co^{II}NIRs indicated that both type 1 and type 2 Cu were replaced with Co^{II}. The metal ion sites have tetrahedral geometries like both Cu^{II} sites of the native enzyme; the Co^{II}-substituted type 1 Cu and type 2 Cu sites have four amino acid residues (2His, Cys, and Met) and three His residues with one water, respectively. The Co^{II}NIRs showed no catalytic activities.

Although many nitrite adducts to Cu^{II} and Cu^{I} complexes have been reported as models for the nitrite-binding active site (the type 2 Cu site) of Cu-NIR [11–18], Co complexes as models for the active site of Co-NIR have been not studied so far. We reported the spectral and structural characterization of Cu^{I} and Cu^{II} complexes containing nitrite and a tridentate aromatic amine (bis(6-methyl-2-pyridylmethyl)amine (Me_2bpa)) as a substrate-binding type 2 Cu site model of nitrite reductase [18]. The coordination modes of the nitrite ligand in $[Cu^{II}(NO_2^-)(ClO_4^-)(Me_2bpa)]$ and $[Cu^{I}(NO_2^-)(Me_2bpa)]_2$ depend on the oxidation state of the Cu, coordinated to Cu^{II} and Cu^{I} through two oxygens (*O*,*O*-coordination) and the nitrogen (*N*-coordination), respectively. The Cu^{I} complex catalyzes the one-electron reduction of nitrite to nitrogen monoxide like Cu-NIR. Herein, we report the spectral and structural characterization of Co^{II} and Co^{III} complexes containing nitrite and tridentate aromatic amines, Me_2bpa and bis(2-pyridylmethyl)amine (bpa) as models of the active site of Co-NIR. The relationship between the binding mode of nitrite to Co^{II} and the catalytic inactivity of the Co^{II}-substituted enzymes will be discussed.

2. Experimental

2.1. *General procedures*

All reagents used in this study are commercial products of the highest available purity and used without purification. Bis(6-methyl-2-pyridylmethyl)amine (Me_2bpa) [19] and bis(2-pyridylmethyl)amine (bpa) [20] were prepared according to previously reported procedures. Infrared spectra were collected with samples prepared as KBr pellets on a JASCO 300E FTIR spectrometer. Electronic absorption spectra were recorded on a JASCO V-570 spectrophotometer at room temperature. Cyclic voltammetric analyses were carried out using a Bioanalytical systems Model CV-50W voltammetric analyzer with a three-electrode system consisting of a $Ag/AgNO_3$ reference electrode, a gold wire counter electrode, and a glassy carbon working electrode under an Ar atmosphere at 25°C. Gas chromatography was performed using a Shimadzu GC14B analyzer with TCD detector (3 m molecular sieve 13X column, helium carrier gas and at 50°C). The nitrite reduction activities were measured according to the previously reported method [15]. An oven-dried Schlenk flask equipped with a magnetic stir bar was evacuated and backfilled with Ar. The flask was charged with a CH_2Cl_2 solution (2 mL)

containing a nitrite-binding Co^{II} complex (**2**, **3**, **4**, or **5**; 8.8–17.5 mmol) (bis(triphenylphosphine)iminium nitrite ($[(Ph_3P)_2N]NO_2$) in the blank experiments) and two equivalent acetic acid at 25.0°C. The product, NO gas, was conducted into a three-necked flask with the constant Ar flow (1 bubble sec^{-1}) through a flexible PVC tube. The three-necked flask was anaerobically filled with 0.1 M aqueous citrate buffer (pH 5.0, 20 mL) containing Na_2EDTA (0.136 mmol) and $FeSO_4 \cdot 7H_2O$ (0.136 mmol) at 5°C. The NO content in aliquots of 2 mL of the Fe complex solution taken by a syringe was monitored by the 432 nm absorbance of [Fe(EDTA)(NO)] ($\varepsilon = 780\ M^{-1}\,cm^{-1}$).

2.2. *Syntheses*

2.2.1. $[Co^{II}(Me_2bpa)Cl_2] \cdot H_2O$ (1). $CoCl_2 \cdot 6H_2O$ (0.5 mmol) was allowed to react with an acetone solution (10 mL) of Me_2bpa (0.5 mmol) for 15 min, giving blue–violet solution. Purple product **1** was crystallized from an acetone solution. Yield approximately 70%. Anal. Calcd for $C_{14}H_{19}N_3O_1Cl_2Co$: C, 44.81; H, 5.11; N, 11.20. Found: C, 44.84; H, 5.06; N, 11.24%.

2.2.2. $[Co^{II}(Me_2bpa)(NO_2)Cl]_2 \cdot$ acetone (2). $CoCl_2 \cdot 6H_2O$ (0.5 mmol) was anaerobically allowed to react with an acetonitrile solution (8 mL) of Me_2bpa (0.5 mmol); to the resulting blue–violet solution was anaerobically added a methanol solution (2 mL) of $NaNO_2$ (0.5 mmol). The color of the mixture changed from blue violet to red violet. After stirring for 15 min, the solution was stored at −20°C overnight. The resulting violet crystals were collected by anaerobic filtration. Yield approximately 35%. Anal. Calcd for $C_{14.5}H_{19}N_4O_{2.5}ClCo$ ($[Co^{II}(Me_2bpa)(NO_2)Cl] \cdot 0.5CH_3OH$): C, 45.38; H, 5.00; N, 14.60. Found: C, 45.21; H, 4.93; N, 14.61%. For X-ray crystal structural analysis, **2** was recrystallized from an acetone/diethyl ether solution.

2.2.3. $Co^{II}(Me_2bpa)(NO_2)_2$ (3). A solution (13 mL) of $NaNO_2$ (1.0 mmol) was anaerobically added to a methanol solution (12 mL) containing $CoCl_2 \cdot 6H_2O$ (0.5 mmol) and Me_2bpa (0.5 mmol). The resulting red-violet solution was allowed to stand overnight at −20°C and red crystals of **3** precipitated. Yield approximately 30%. Anal. Calcd for $C_{14}H_{17}N_5O_4Co$: C, 44.45; H, 4.54; N, 18.52. Found: C, 44.53; H, 4.54; N, 18.34%.

2.2.4. $[Co^{II}(bpa)(NO_2)Cl]$ (4). $CoCl_2 \cdot 6H_2O$ (0.5 mmol) was anaerobically reacted with an ethanol solution (6 mL) of bpa (0.5 mmol); to the resulting blue-violet solution was anaerobically added a methanol solution (2 mL) of $[(Ph_3P)_2N]NO_2$ (0.5 mmol). The color of the mixture changed from blue violet to red violet. After stirring for 15 min, the resulting violet crystals were collected by anaerobic filtration. Yield approximately 70%. Anal. Calcd for $C_{14}H_{19}N_4O_3ClCo$ ($[Co^{II}(bpa)(NO_2)Cl] \cdot C_2H_5OH$): C, 43.59; H, 4.97; N, 14.53. Found: C, 43.79; H, 4.46; N, 14.32%. Vis – near IR (λ_{max} nm ($\varepsilon\ mol^{-1}\,cm^{-1}$) in acetone): 510 (125), 650 (shoulder), 1040 (11). Recrystallized single crystals of **4** contained no ethanol.

2.2.5. $Co^{II}(bpa)(NO_2)_2$ (5). $CoCl_2 \cdot 6H_2O$ (1.0 mmol) was anaerobically reacted with a methanol solution (2 mL) of bpa (1.0 mmol); to the resulting blue-violet solution was anaerobically added a methanol solution (10 mL) of $NaNO_2$ (4.0 mmol). The color of the mixture changed from blue violet to red violet. After stirring for 30 min, pink powder of **5** was collected by anaerobic filtration. The pink product was recrystallized from deoxygenated methanol. Yield approximately 13%. Anal. Calcd for $C_{12}H_{13}N_5O_4Co$: C, 41.15; H, 3.75; N, 20.00. Found: C, 41.02; H, 3.78; N, 19.81%. Vis – near IR (λ_{max} nm (ε $M^{-1}\,cm^{-1}$) in acetone): 490 (72), 565 (75), 940 (7).

2.2.6. $Co^{III}(Me_2bpa)(NO_2)(CO_3)$ (6). An aqueous solution (2 mL) containing $K_3[Co(CO_3)_3]$ [21] (1 mmol) was added to a solution of Me_2bpa (1 mmol) in water (2 mL). When the resulting solution was stirred with 3 mL of 2 mmol aqueous acetic acid, the solution changed to black. A solution of $NaNO_2$ (5 mmol) in water (2 mL) was added to the black solution and stirred overnight, giving a brown-red solution containing pale red crystals of **6**. The crystals were filtered off, washed with a small amount of water, and air-dried. Yield approximately 46%. Anal. Calcd for $C_{15}H_{17}N_4O_5Co$: C, 45.92; H, 4.38; N, 14.29. Found: C, 45.04; H, 4.44; N, 14.22%. Vis (λ_{max} nm (ε $mmol^{-1}\,cm^{-1}$) in 5 mmol acetic acid): 510 (210).

2.2.7. $Co^{III}(bpa)(NO_2)_3$ (7). An aqueous solution (5 mL) of NaOH (7 mmol) was added to an aqueous solution containing $CoCl_2 \cdot 6H_2O$ (1 mmol) and $NaNO_2$ (5 mmol). The resulting solution containing a blue precipitate was treated with acetic acid at pH 6 giving a homogeneous orange solution. A solution containing bpa (1 mmol) in water (2 mL) was added dropwise to the aerated orange solution. After 3 h aeration, orange crystals of **7** were filtered off, washed with water, and dried in air. Yield approximately 30%. Anal. Calcd for $C_{12}H_{13}N_6O_6Co$: C, 36.37; H, 3.31; N, 21.21. Found: C, 36.38; H, 3.26; N, 21.08%. Vis (λ_{max} nm (ε $mol^{-1}\,cm^{-1}$) in 5 mol acetic acid): 480 (240).

2.3. *Crystallography*

For X-ray crystal structure analyses of **1**, **2**, **4**, **6**, and **7**, intensity data were collected at room temperature on a Mac Science MXC3 diffractometer. Reflection data for **3** were collected at room temperature using a Rigaku Mercury diffractometer and a Rigaku AFC-7R diffractometer equipped with a Rigaku Mercury CCD area detector. All crystals of **1**–**7** were mounted to a glass capillary. Graphite monochromated Mo-Kα radiation was used in all cases. The structures were solved by direct methods and refined by full-matrix least-squares on F^2_{obs} with anisotropic thermal parameters for all non-hydrogen atoms. All structures were solved by direct methods and refined anisotropically for non-hydrogen atoms by full-matrix least-squares calculations. The programs CRYSTAN-GM [22] and Crystal Structure were used for data reduction, structure solution, and structure refinement; molecular graphics were created by ORTEP. The crystal and refinement details for **1**, **2**, **3**, **4**, **6**, and **7** are listed in table 1.

Table 1. Crystallographic data for $[Co^{II}(Me_2bpa)Cl_2]\cdot H_2O$ (**1**), $[Co^{II}(Me_2bpa)(NO_2)Cl]_2\cdot$acetone (**2**), $Co^{II}(Me_2bpa)(NO_2)_2$ (**3**), $Co^{II}(bpa)(NO_2)Cl$ (**4**), $Co^{III}(Me_2bpa)(NO_2)(CO_3)$ (**6**), and $Co^{III}(bpa)(NO_2)_3$ (**7**).

	1	**2**	**3**	**4**	**6**	**7**
Empirical formula	$C_{14}H_{19}N_3OCl_2Co$	$C_{31}H_{40}N_8O_5Cl_2Co_2$	$C_{14}H_{17}N_5O_4Co$	$C_{12}H_{13}N_4O_2ClCo$	$C_{15}H_{17}N_4O_5Co$	$C_{12}H_{13}N_6O_6Co$
Formula weight	375.19	793.55	378.29	339.67	392.29	396.24
Color	Blue	Purple	Red	Purple	Red	Orange
Crystal size (mm)	$4.0\times1.5\times1.2$	$0.35\times0.2\times0.1$	$1.5\times0.3\times0.3$	$0.7\times0.36\times0.3$	$3.0\times1.0\times0.8$	$0.3\times0.3\times0.05$
Crystal system	Monoclinic	Monoclinic	Monoclinic	Monoclinic	Triclinic	Monoclinic
Space group	*P2(1)/n*	*P2(1)/c*	*P2(1)/a*	*P2(1)/a*	*P1*	*P2(1)*
Unit cell dimensions (Å, °)						
a	16.839(5)	7.8416(9)	15.330(2)	13.78(2)	8.785(2)	9.625(2)
b	11.494(3)	32.705(5)	11.960(2)	7.966(3)	12.484(1)	8.896(3)
c	8.596(2)	14.543(2)	8.652(1)	13.140(5)	7.978(3)	8.7866(8)
α	–	–	–	–	91.49(2)	–
β	93.23(2)	97.667(5)	94.78(1)	96.15(7)	116.84(2)	93.57(1)
γ	–	–	–	–	97.28(1)	–
Volume (Å^3), *Z*	1661.1(8), 4	3696.2(8), 8	1580.8(4), 4	1434(2), 4	770.9(3), 2	750.9(3), 2
Calculated density (g cm^{-3})	1.500	1.426	1.589	1.700	1.728	1.743
Radiation	Mo-Kα ($\lambda=0.71073$)	Mo-Kα ($\lambda=0.71073$)	Mo-Kα ($\lambda=0.71073$)	Mo-Kα ($\lambda=0.71073$)	Mo-Kα ($\lambda=0.71073$)	Mo-Kα ($\lambda=0.71073$)
Absorption coefficient (mm^{-1})	1.356	1.091	1.116	1.386	1.159	1.190
Crystal size (mm^3)	$4.0\times1.5\times1.2$	$0.35\times0.2\times0.1$	$1.5\times0.3\times0.3$	$0.7\times0.36\times0.3$	$3.0\times1.0\times0.8$	$0.3\times0.3\times0.05$
Reflections collected	2649	4028	2127	2344	2317	1563
R^a	0.048	0.058	0.043	0.050	0.049	0.041
R_w^b	0.064	0.046	0.034	0.068	0.064	0.054

[a] $R=\sum||F_o|-|F_c||/\sum|F_o|$, [b] $R_w=\{\sum w(|F_o|-|F_c|)^2/\sum wF_o^2\}^{1/2}$; **1**, $w=1/\{\sigma^2(F_o)+0.001(F_o)^2\}$; **2** and **3**, $w=w=1/\{\sigma^2(F_o)\}$; **4**, **6**, and **7**, $w=1/\{\sigma^2(F_o)+0.03(F_o)^2\}$.

3. Results and discussion

3.1. *Electronic absorption spectra of 1, 2, and 3*

Figure 1 shows the visible and near-infrared absorption spectra of the three Co(II) complexes (**1**, **2**, and **3**) containing Me_2bpa in acetone. For $Co(Me_2bpa)Cl_2$ (**1**) the bands at 540, 590–620, 820, and 1030 nm can be correlated with the bands for $Co(dienMe)Cl_2$ (dienMe, bis(2-dimethylaminoethyl)methylamine) at 532, 621, 943, and 1150 nm in chloroform [23], which are explained by a trigonal bipyramidal crystal field model [24]. The $Co^{II}(Me_2bpa)(NO_2)Cl$ complex in **2** and $Co^{II}(Me_2bpa)(NO_2)_2$ (**3**) exhibit bands at 540 and 1020 nm, and 530 and 920 nm, respectively. The 530–540 nm and near-infrared bands can be assigned to the $^4T_{1g}(F) \rightarrow {}^4T_{1g}(P)$ or $^4A_{2g}$ and $^4T_{1g}(F) \rightarrow {}^4T_{2g}$ transition for high-spin octahedral complexes [25]. Co^{II} complexes (**4** and **5**) containing bpa and NO_2^- also have visible and near-infrared absorption bands (**4**: 510 and 1040 nm; **5**: 490, 565, and 940 nm in acetone), which suggest high-spin octahedral Co(II).

3.2. *Structure of $Co^{II}(Me_2bpa)Cl_2$ complex containing no nitrite ligand (1)*

The X-ray crystal structure of **1** is depicted in figure 2 and elected bond distances and angles are listed in table 2. The Co^{II} in **1** shows a distorted trigonal bipyramidal geometry with three nitrogens of Me_2bpa and two chlorides. The bond lengths Co–N(1) and Co–N(3) were 2.163(5) and 2.193(5) Å, respectively, slightly longer than the $Co–N_{py}$ lengths of $[Co^{II}(terpy)Cl_2]$ (2.09–2.17 Å) [26]. A Co^{II} complex with bpa and chloride has been reported by Davies *et al*. [27] as a μ-dichloro dimer $[(fac\text{-bpa})Co^{II}Cl(\mu\text{-}Cl)]_2$. The cobalt centers are bridged by two chlorides and bound terminally by a chloride and a bpa to give a distorted octahedral geometry at each cobalt.

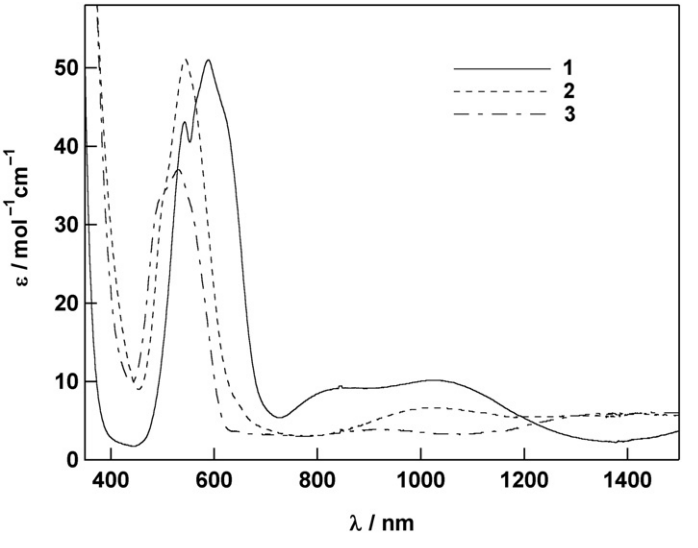

Figure 1. Electronic absorption spectra of **1**, **2**, and **3** in acetone.

The monomeric structure of **1** may be due to the steric hindrance of the methyl groups at 6-position of pyridine in Me_2bpa.

3.3. *Structures of $Co^{II}Me_2bpa$ and $Co^{II}bpa$ complexes containing one nitrite ion (2 and 4)*

The X-ray crystal structures of $[Co^{II}(Me_2bpa)(NO_2)Cl]$ and $[Co^{II}(bpa)(NO_2)Cl]$ (**2** and **4**) are depicted in figure 3 and their selected bond distances and angles are listed in tables 3 and 4. For **2**, from a mixture of acetone and diethyl ether, two Co complexes and one acetone exist in the unit cell (figure S1). The structure of **2** containing distorted octahedral Co^{II} reveals replacement of one Cl^- in **1** with a nitrite showing asymmetric *O*,*O*′-nitrito chelation. The equatorial O(2) forms an equatorial plane with the three nitrogens of Me_2bpa and O(1) axially binds to Co^{II}. Complex **2** exhibits two distinct Co^{II}–$O_{nitrite}$ bond lengths (Co(1)–O(1) = 2.267(5) Å,

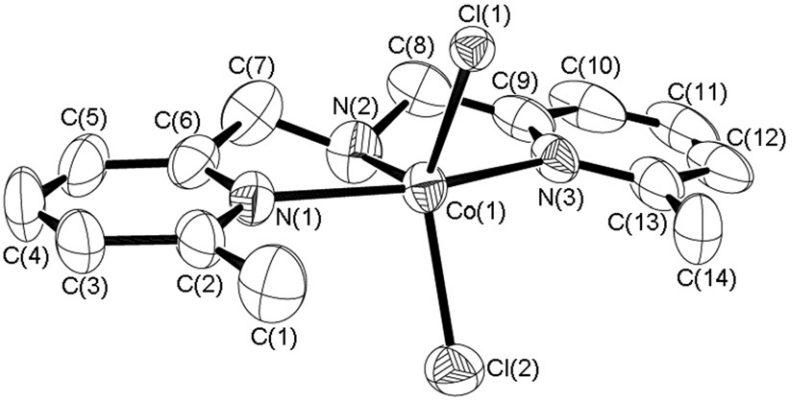

Figure 2. ORTEP plot of $[Co^{II}(Me_2bpa)Cl_2]$ in **1** with 50% probability thermal ellipsoids. The hydrogens have been omitted for clarity.

Table 2. Selected bond lengths (Å) and angles (°) for **1** with estimated standard deviations in parentheses.

Bond length (Å)		Bond angle (°)	
Co(1)–Cl(1)	2.311(2)	Cl(1)–Co(1)–Cl(2)	129.4(1)
Co(1)–Cl(2)	2.306(2)	Cl(1)–Co(1)–N(1)	96.2(2)
Co(1)–N(1)	2.193(5)	Cl(1)–Co(1)–N(2)	121.3(2)
Co(1)–N(2)	2.075(6)	Cl(1)–Co(1)–N(3)	94.0(2)
Co(1)–N(3)	2.162(5)	Cl(2)–Co(1)–N(1)	95.0(2)
		Cl(2)–Co(1)–N(2)	109.3(2)
		Cl(2)–Co(1)–N(3)	93.9(2)
		N(1)–Co(1)–N(2)	78.6(2)
		N(1)–Co(1)–N(3)	157.5(2)
		N(2)–Co(1)–N(3)	79.0(3)
		Cl(1)–Co(1)–N(1)	96.2(2)

Co(1)–O(2) = 2.093(6) Å, Co(2)–O(21) = 2.286(5) Å, Co(2)–O(22) = 2.073(6) Å) and two distinct N–O bond lengths (N(4)–O(1) = 1.231(8) Å, N(4)–O(2) = 1.198(7) Å, N(24)–O(21) = 1.256(7) Å, and N(24)–O(22) = 1.189(7) Å). The O–N–O angles of nitrite (O(1)–N(4)–O(2) = 116.3(8)° and O(21)–N(24)–O(22) = 114.4(8)) are similar to those in free nitrite (O–N–O = 114.9(5)°). The coordination mode of nitrite in **2** is similar to those in $[Cu^{II}Me_2bpa(NO_2)(ClO_4)]$ (Cu–O = 2.47(3) and 1.98(2) Å), which is the model complex for the active site of Cu-NIR [18] and the nitrite-binding type 2 Cu^{II} site in nitrite-soaked Cu-NIR (Cu–O = 2.29–2.38, 2.04–2.08 Å) [7]. Complex **4** also has a distorted octahedral geometry with three nitrogens of bpa *fac*, chloride, and two oxygens of nitrite. The Co–$N(1)_{py}$ and Co–$N(3)_{py}$ bond lengths (2.116(5) and 2.114(4) Å, respectively) in **4** were slightly shorter than in **2** (2.16–2.21 Å). Although the Co^{II} ion was situated in N(1)N(2)N(3) plane of Me_2bpa ligand, Co^{II} ion was not

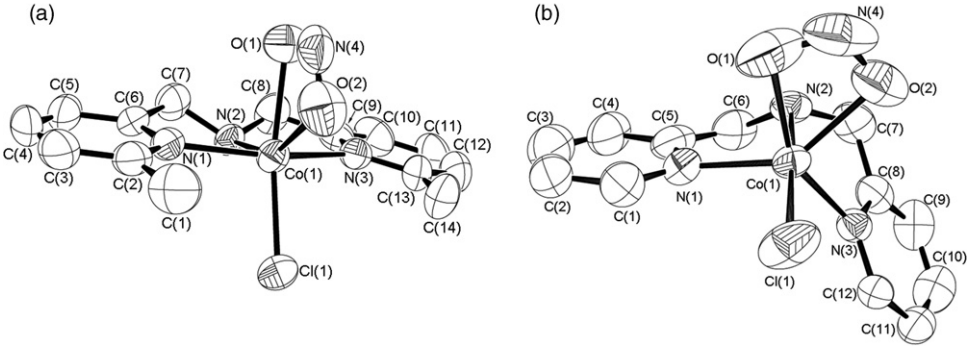

Figure 3. ORTEP plots of (a) $[Co^{II}(Me_2bpa)(NO_2)Cl]$ in **2** and (b) $[Co^{II}(bpa)(NO_2)Cl]$ (**4**) with 50% probability thermal ellipsoids. The hydrogens have been omitted for clarity.

Table 3. Selected bond lengths (Å) and angles (°) for **2** with estimated standard deviations in parentheses.

	Bond length (Å)		Bond angle (°)		Bond angle (°)
Co(1)–Cl(1)	2.336(2)	Cl(1)–Co(1)–O(1)	162.9(2)	Cl(2)–Co(2)–O(21)	164.9(2)
Co(1)–O(1)	2.267(5)	Cl(1)–Co(1)–N(1)	95.8(1)	Cl(2)–Co(2)–N(21)	95.6(2)
Co(1)–O(2)	2.093(6)	Cl(1)–Co(1)–N(2)	108.6(1)	Cl(2)–Co(2)–O(22)	108.9(2)
Co(1)–N(1)	2.183(5)	Cl(1)–Co(1)–N(3)	94.7(1)	Cl(2)–Co(2)–N(23)	95.0(1)
Co(1)–N(2)	2.074(5)	O(1)–Co(1)–N(1)	88.3(2)	O(21)–Co(2)–N(21)	87.6(2)
Co(1)–N(3)	2.214(5)	O(1)–Co(1)–N(2)	88.5(2)	O(21)–Co(2)–N(22)	88.2(2)
Co(2)–Cl(2)	2.338(2)	O(1)–Co(1)–N(3)	87.2(2)	O(21)–Co(2)–N(23)	87.2(2)
Co(2)–O(21)	2.286(5)	N(1)–Co(1)–N(2)	79.5(2)	N(21)–Co(2)–N(22)	79.3(2)
Co(2)–O(22)	2.073(6)	N(2)–Co(1)–N(3)	78.9(2)	N(22)–Co(2)–N(23)	79.0(2)
Co(2)–N(21)	2.168(5)	N(1)–Co(1)–N(3)	158.0(2)	N(21)–Co(2)–N(23)	157.8(2)
Co(2)–N(22)	2.076(5)	O(2)–Co(1)–N(1)	98.0(2)	O(22)–Co(2)–N(21)	98.9(2)
Co(2)–N(23)	2.189(5)	O(2)–Co(1)–N(2)	144.8(2)	O(22)–Co(2)–N(22)	144.2(2)
O(1)–N(4)	1.231(8)	O(2)–Co(1)–N(3)	97.4(2)	O(22)–Co(2)–N(23)	96.1(2)
O(2)–N(4)	1.198(7)	O(1)–Co(1)–O(2)	56.3(2)	O(21)–Co(2)–O(22)	56.0(2)
O(21)–N(24)	1.256(7)	Co(1)–O(1)–N(4)	89.0(5)	Co(2)–O(21)–N(24)	88.5(5)
O(22)–N(24)	1.189(7)	Co(1)–O(2)–N(4)	98.4(6)	Co(2)–O(22)–N(24)	101.0(5)
		Cl(1)–Co(1)–O(2)	106.7(2)	Cl(2)–Co(2)–N(22)	106.8(2)
		O(1)–N(4)–O(2)	116.3(8)	O(21)–N(24)–O(22)	114.4(8)

located in the plane of bpa. Moreover, Co, N(4), and two O (1 and 2) atoms in **2** lie in the same plane, but not in **4**. The structural difference between **2** and **4** is ascribable to the methyl groups at the 6-position of pyridine in Me_2bpa. The N–O bond lengths (N(4)–O(1) = 1.247(1) Å, N(4)–O(2) = 1.225(9) Å, and the O–N–O angle of nitrite (O(1)–N(4)–O(2) = 113.8(6)°) in **4** are similar to those in a free nitrite [28] and $[Cu^{II}Me_2bpa(NO_2)(ClO_4)]$ (N–O = 1.24(4) and 1.28(4) Å and O–N–O = 115.8(3)°) [18].

IR spectra of **2** and **4** display characteristic bands of the nitrite groups: $\nu_a(NO_2)$ at 1222 cm^{-1} [$\nu_a(^{15}NO_2)$ at 1184 cm^{-1}], $\nu_s(NO_2)$ at 1202 cm^{-1} [$\nu_s(^{15}NO_2)$ at 1158 cm^{-1}] for **2** and $\nu_a(NO_2)$ at 1217 cm^{-1} [$\nu_a(^{15}NO_2)$ at 1179 cm^{-1}], $\nu_s(NO_2)$ at 1198 cm^{-1} [$\nu_s(^{15}NO_2)$ at 1149 cm^{-1}] for **4**. In general, the two vibrations of monodentate nitrito complexes (*O*-coordination) are well separated: ν (N=O) and ν (N–O) in the 1485–1400 and 1110–1050 cm^{-1} region, respectively [29]. Moreover, when nitrito group is chelating (*O*,*O*-coordination) the $\nu_a(NO_2)$ and $\nu_s(NO_2)$ of the chelating nitrite group will be shifted to a lower and a higher frequency, respectively, relative to those of *O*-coordination complexes. The separation between these two modes ($\nu_a(NO_2)$ and $\nu_s(NO_2)$) becomes much smaller than those of monodentate complexes. For example, $Co(Ph_3PO)_2(NO_2)_2$, in which nitrite is chelating, exhibits the ν_a and ν_s at 1266 and 1199 cm^{-1}, respectively [29]. The coordination modes based on IR signals of **2** and **4** are consistent with those of their X-ray crystal structures.

3.4. *Structure of $Co^{II}Me_2bpa$ and $Co^{II}bpa$ complexes containing two nitrite ions (3 and 5)*

Complex **3** has a distorted octahedral geometry with three nitrogens of Me_2bpa *mer*, two oxygens of one nitrite, and one of two oxygens of another nitrite (figure 4 and table 5). The former nitrite is asymmetric bidentate *via* both of its oxygens. Although the bond length (2.080(4) Å) between Co^{II} and equatorial O(2) of bidentate

Table 4. Selected bond lengths (Å) and angles (°) for **4** with estimated standard deviations in parentheses.

Bond length (Å)		Bond angle (°)	
Co(1)–Cl(1)	2.329(2)	Cl(1)–Co(1)–N(1)	100.5(2)
Co(1)–N(1)	2.116(5)	Cl(1)–Co(1)–N(2)	172.8(2)
Co(1)–N(2)	2.182(4)	Cl(1)–Co(1)–N(3)	98.1(1)
Co(1)–N(3)	2.114(4)	Cl(1)–Co(1)–O(1)	93.3(2)
Co(1)–O(1)	2.250(6)	Cl(1)–Co(1)–O(2)	99.8(2)
Co(1)–O(2)	2.161(5)	N(1)–Co(1)–N(2)	77.0(2)
N(4)–O(1)	1.246(11)	N(1)–Co(1)–N(3)	110.9(2)
N(4)–O(2)	1.225(9)	N(1)–Co(1)–O(1)	91.6(3)
		N(1)–Co(1)–O(2)	142.5(2)
		N(2)–Co(1)–N(3)	76.7(2)
		N(2)–Co(1)–O(1)	93.5(2)
		N(2)–Co(1)–O(2)	85.9(2)
		N(3)–Co(1)–O(1)	152.2(2)
		N(3)–Co(1)–O(2)	97.0(2)
		O(1)–Co(1)–O(2)	56.0(3)
		O(1)–N(4)–O(2)	113.8(6)
		Co(1)–O(1)–N(4)	92.6(5)
		Co(1)–O(2)–N(4)	97.6(5)

nitrite in **3** is almost the same as that in **2** (2.093(6) and 2.073(6) Å), the bond length (2.412 Å) between Co^{II} ion and axial O(1) coordinating atom of bidentate nitrite ligand in **3** is longer than that in **2** (2.267(5) and 2.286(5) Å). The O(1)–Co–O(2) angle (53.9°) of nitrite in **3** raises the O(2) coordination position from the equatorial plane of the Co^{II}, which is composed of the N(1), N(2), and N(3). The O(1)–N(4)–O(2) angle (112°) of the chelating nitrite in **3** is similar to O–N–O angle (114.9(5)°) of free nitrite [28]. The difference between two N–O bond lengths of bidentate nitrite in **3** (N(4)–O(1) = 1.252(4) Å and N(4)–O(2) = 1.234(4) Å) is smaller than that in **2**. This suggests that the electron density of the nitrite is delocalized on the ligand. IR spectra of **3** display characteristic bands of nitrite, ν (N=O) at 1341 cm^{-1} [$\nu(^{15}N{=}O)$ at 1323 cm^{-1}], $\nu_a(NO_2)$ at 1272 cm^{-1} [$\nu_a(^{15}NO_2)$ at 1241 cm^{-1}] and $\nu_s(NO_2)$ at 1197 cm^{-1}

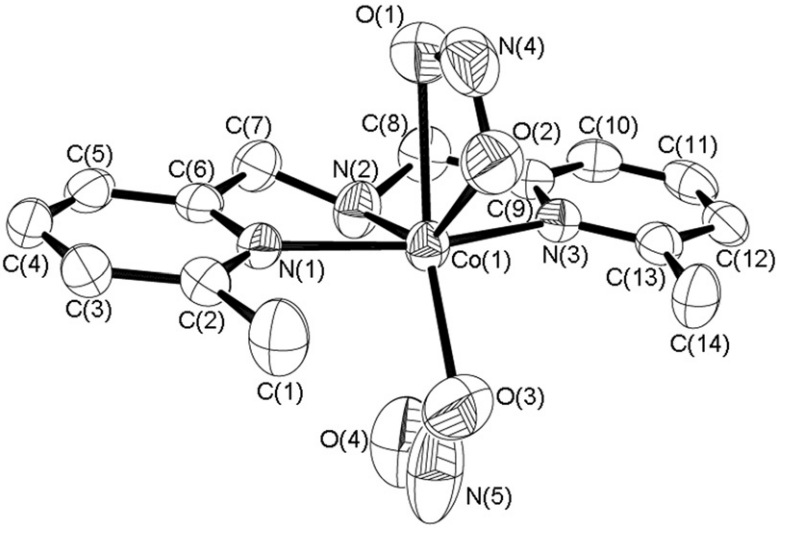

Figure 4. ORTEP plot of $Co^{II}(Me_2bpa)(NO_2)_2$ (**3**) with 50% probability thermal ellipsoids. The hydrogens have been omitted for clarity.

Table 5. Selected bond lengths (Å) and angles (°) for **3** with estimated standard deviations in parentheses.

Bond length (Å)		Bond angle (°)	
Co(1)–N(1)	2.149(3)	N(1)–Co(1)–N(2)	80.28(13)
Co(1)–N(2)	2.082(3)	N(2)–Co(1)–N(3)	79.58(13)
Co(1)–N(3)	2.145(3)	N(1)–Co(1)–N(3)	159.40(11)
Co(1)–O(1)	2.412(3)	N(1)–Co(1)–O(3)	95.22(15)
Co(1)–O(2)	2.105(3)	O(1)–Co(1)–O(2)	53.9(1)
Co(1)–O(3)	2.080(4)	O(1)–Co(1)–O(3)	153.3(2)
N(4)–O(1)	1.252(4)	O(2)–Co(1)–O(3)	99.63(16)
N(4)–O(2)	1.234(4)	O(1)–N(4)–O(2)	112.3(4)
N(5)–O(3)	1.118(7)	O(3)–N(5)–O(4)	117.5(9)
N(5)–O(4)	1.081(6)		

[$\nu_s(^{15}NO_2)$ at 1177 cm^{-1}]. The $\nu_a(NO_2)$ and $\nu_s(NO_2)$ bands are assigned to vibrations of the bidentate nitrite, while the ν(N=O) band is due to the monodentate nitrite compared with monodentate nitrite complex (*O*-coordination); $[Co^{II}(py)_4(ONO)_2](py)_2$ (1405 cm^{-1}) [29]. Single crystals of **5** have not been obtained. From IR spectra of **5**, however, we speculated that the structure of **5** is very similar to that of **3**. The IR spectra of **5** display characteristic bands of nitrite at 1205, 1228, and 1308 cm^{-1}, which were shifted to 1178, 1200, and 1284 cm^{-1}, respectively, in **5** containing $^{15}NO_2^-$ ions. In comparison with IR data of **3**, the 1205 and 1228 cm^{-1} bands would be assigned to bidentate nitrite ($\nu_s(NO_2)$ and $\nu_a(NO_2)$, respectively) and the 1308 cm^{-1} band would be due to a monodentate nitrite. Therefore, **5** would have a distorted octahedral geometry with three nitrogens of bpa, two oxygens (bidentate *O*,*O*′-coordination) of nitrite, and one of two oxygens (monodentate *O*-coordination) of another nitrite.

3.5. *Structure of $Co^{III}Me_2bpa$ and $Co^{III}bpa$ complexes containing nitrite (6 and 7)*

The X-ray crystal structures of **6** and **7** are shown in figure 5 and their selected bond distances and angles are tabulated in tables 6 and 7. Both complexes adopt slightly distorted octahedral geometries with three nitrogens of Me_2bpa *fac*, two oxygens of carbonate, and one nitrogen of nitrite in **6**, and three nitrogens of bpa *mer* and each nitrogen of three nitrites in **7**. All nitrites in **6** and **7** are *N*-coordinated and all Co^{III}–N distances are 1.93–1.97 Å. The average N–O bond length (1.23 Å) of the nitrites is from 1.21 to 1.26 Å of the several nitrite-binding Co^{III} complexes [30–34]; only N(6)–O(6) (1.19 Å) in **7** is out of the range. All O–N–O angles of the nitrito are 118–120°. IR spectra of **6** and **7** show characteristic stretching frequencies [$\nu_a(NO_2)$ and $\nu_s(NO_2)$ in the 1470–1370 and 1340–1320 cm^{-1} region, respectively [29]] of *N*-coordinated nitrite complexes: $\nu_a(NO_2)$ at 1397 cm^{-1} [$\nu_a(^{15}NO_2)$ at 1371 cm^{-1}] and $\nu_s(NO_2)$ at 1308 cm^{-1} [$\nu_s(^{15}NO_2)$ at 1285 cm^{-1}] for **6**; $\nu_a(NO_2)$ at 1400 cm^{-1} [$\nu_a(^{15}NO_2)$ at 1384 cm^{-1}] and $\nu_s(NO_2)$ at 1304 cm^{-1} [$\nu_s(^{15}NO_2)$ at 1283 cm^{-1}] for **7**. The *N*-coordination modes based on the IR signals of **6** and **7** are consistent with those of their X-ray crystal structures.

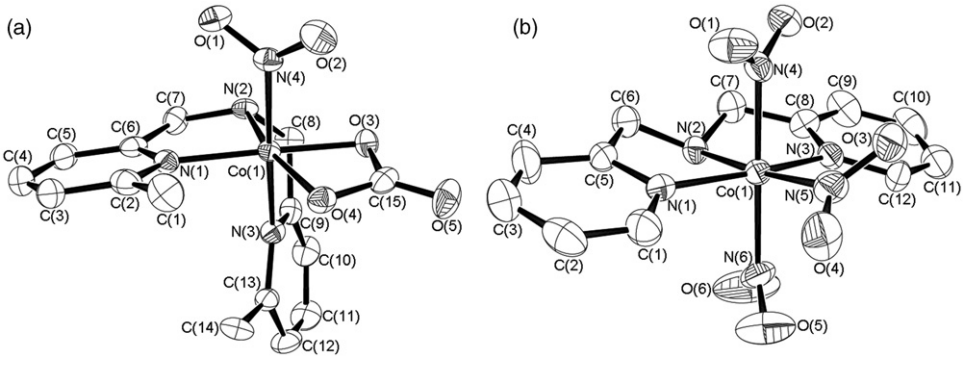

Figure 5. ORTEP plots of (a) $Co^{III}(Me_2bpa)(NO_2)(CO_3)$ (**6**) and (b) $Co^{III}(bpa)(NO_2)_3$ (**7**) with 50% probability thermal ellipsoids. The hydrogens have been omitted for clarity.

Table 6. Selected bond lengths (Å) and angles (°) for **6** with estimated standard deviations in parentheses.

	Bond length (Å)		Bond angle (°)
Co(1)–N(1)	1.963(6)	N(1)–Co(1)–N(2)	85.9(3)
Co(1)–N(2)	1.949(6)	N(2)–Co(1)–N(3)	81.3(3)
Co(1)–N(3)	2.000(6)	N(3)–Co(1)–N(4)	173.7(3)
Co(1)–N(4)	1.925(6)	N(1)–Co(1)–O(4)	108.9(3)
Co(1)–O(3)	1.882(5)	N(4)–Co(1)–O(3)	90.3(3)
Co(1)–O(4)	1.925(5)	N(4)–Co(1)–O(4)	91.5(3)
N(4)–O(1)	1.256(8)	O(3)–Co(1)–O(4)	69.0(2)
N(4)–O(2)	1.220(8)	O(1)–N(4)–O(2)	119.2(6)

Table 7. Selected bond lengths (Å) and angles (°) for **7** with estimated standard deviations in parentheses.

	Bond length (Å)		Bond angle (°)
Co(1)–N(1)	1.95(3)	N(1)–Co(1)–N(2)	82.2(16)
Co(1)–N(2)	1.95(4)	N(2)–Co(1)–N(3)	83.1(6)
Co(1)–N(3)	1.954(17)	N(3)–Co(1)–N(4)	92.8(6)
Co(1)–N(4)	1.957(5)	N(1)–Co(1)–N(3)	165.2(21)
Co(1)–N(5)	1.96(4).	N(2)–Co(1)–N(4)	91.6(12)
Co(1)–N(6)	1.966(6)	N(5)–Co(1)–N(6)	94.4(13)
N(4)–O(1)	1.234(7)	O(1)–N(4)–O(2)	120.3(5)
N(4)–O(2)	1.229(7)	O(3)–N(5)–O(4)	118.9(8)
N(5)–O(3)	1.252(9)	O(5)–N(6)–O(6)	117.8(7)
N(5)–O(4)	1.216(10)		
N(6)–O(5)	1.217(11)		
N(6)–O(6)	1.191(12)		

3.6. *Nitrite reduction activities of Co complexes*

Our previous article reported that $[Cu^{I}(Me_2bpa)(NO_2)]$ reacts with two equivalents of acetic acid to yield NO and $Cu^{II}(Me_2bpa)$ acetate under anaerobic conditions [18]. To investigate nitrite reduction activity of the nitrite-binding Co^{II} complexes as a model for the reaction center in Co^{II}NIR, we examined the reactions of **2**, **3**, **4**, and **5** with acetic acid. When two equivalents of acetic acid to nitrite ligand were added to CH_2Cl_2 solutions of **2**, **3**, **4**, and **5** at 25.0°C, the colors of the solutions hardly changed. Evolution of NO gas can be confirmed by reaction with [Fe(EDTA)] solution; NO gas evolved by the reactions of **2**, **3**, **4**, and **5** with acetic acid could be monitored by the 432 nm absorbance of [Fe(EDTA)(NO)]. However, NO gas was not observed. Moreover, no N_2O gas was detected by a gas chromatography. These findings suggest that nitrite binding to Co^{II} cannot react with proton to produce NO and N_2O. In the nitrite reduction of $[Cu^{I}(Me_2bpa)(NO_2)]$, *N*-coordination of nitrite to the type 2 Cu^{I} center and protonation to oxygen of the nitrite have been proposed as key points of the nitrite reduction [18]. However, according to the X-ray crystal and IR data of **2**, **3**, **4**, and **5** nitrite show *O*- and *O*,*O*′-coordination. These results suggest that the nitrito coordination of nitrite in **2**, **3**, **4**, and **5** suppresses protonation of the nitrite

preventing reductions. The $Cu^{II}(Me_2bpa)$ complex was able to be electrochemically reduced to the Cu^{I} species. When the Cu^{II} complex was reduced in the presence of nitrite and proton (acetic acid), the observed catalytic current suggested reduction of nitrite by the reduced Cu complex [18]. Therefore, we tried electrochemical reductions of **2**, **3**, **4**, and **5** to produce the corresponding Co^{I} species in CH_2Cl_2 solution. However, these Co^{II} complexes were not reduced in the range 0.5 to −2.0 V *versus* $Ag/AgNO_3$ at 25°C in the presence or absence of proton, suggesting that the redox potentials (Co^{I}/Co^{II}) of **2**, **3**, **4**, and **5** might be shifted negatively and their Co^{I} complexes with the Me_2bpa and nitrite ligands might be unstable. These findings imply that Co^{II}NIR has no enzymatic activity.

4. Conclusions

Co^{II} and Co^{III} complexes containing nitrite and Me_2bpa or bpa have been synthesized and characterized structurally. The coordination modes of nitrite ligands were dependent on the cobalt oxidation states, coordinated to Co^{II} through the oxygen (*O*- and *O*,*O*′-coordination mode, and to Co^{III} through nitrogen (*N*-coordination mode). The binding modes of nitrite were quite different from those of Cu complexes containing nitrite and Me_2bpa ligands where nitrite coordinates to Cu^{II} and Cu^{I} through two oxygens (*O*,*O*′-coordination mode) and one nitrogen (*N*-coordination mode), respectively. These findings indicate that the nitrogen of nitrite ion has an affinity, both for the typical hard acid Co(III) and for the typical soft acid Cu(I), because *N*-coordinated nitrite is a borderline base. Although $[Cu^{I}(Me_2bpa)(NO_2)]$ reacts with proton to produce NO in nitrite reduction, the nitrite-binding Co^{II} complexes did not. The nitrite ion bound to Co^{II} complexes in *O*- and *O*,*O*′-coordination modes might be unreactive with protons needed for reduction to NO. Moreover, the instability of the nitrite-binding Co^{I} complexes might cause no enzymatic activity of Co^{II}NIR.

Supplementary material

Crystallographic data for the structures reported in this article have been deposited with the Cambridge Crystallographic Data Centre: Deposition numbers CCDC-741304 for **1**, CCDC-741305 for **2**, CCDC-741306 for **3**, CCDC-741307 for **4**, CCDC-741308 for **6**, and CCDC-741309 for **7**. Copies of the data can be obtained free of charge *via* http://www.ccdc.cam.ac.jp/conts/retrieving.html (or from the Cambridge Crystallographic Data Centre, 12 Union Road, Cambridge, CB2 1EZ, UK; Fax: 44 11223 336033; Email: deposit@ccdc.cam.ac.uk).

References

[1] S. Suzuki, K. Kataoka, K. Yamaguchi, T. Inoue, Y. Kai. *Coord. Chem. Rev.*, **190–192**, 245 (1999).
[2] S. Suzuki, K. Kataoka, K. Yamaguchi. *Acc. Chem. Res.*, **33**, 728 (2000).
[3] E.T. Adman, J.W. Godden, S. Turley. *J. Biol. Chem.*, **270**, 27458 (1995).

[4] M.E.P. Murphy, S. Turley, E.T. Adman. *J. Biol. Chem.*, **272**, 28455 (1997).
[5] F.E. Dodd, J.V. Beeumen, R.R. Eady, S.S. Hasnain. *J. Mol. Biol.*, **282**, 369 (1998).
[6] M. Nojiri, H. Koteishi, T. Nakagami, K. Kobayashi, T. Inoue, K. Yamaguchi, S. Suzuki. *Nature*, **462**, 117 (2009).
[7] E.L. Tocheva, F.I. Rosell, A.G. Mauk, M.E.P. Murphy. *Science*, **304**, 867 (2004).
[8] S. Suzuki, Deligeer, K. Yamaguchi, K. Kataoka, S. Shidara, H. Iwasaki, T. Sakurai. *Inorg. Chim. Acta*, **275–276**, 289 (1998).
[9] S. Suzuki, T. Sakurai, A. Nakahara, M. Sasuko, H. Iwasaki. *Biochem. Biophys. Acta*, **827**, 190 (1985).
[10] B.L. Vallee, B. Holmquist. In *Advances in Inorganic Biochemistry: Methods for Determining Metal Ion Environments in Proteins*, D.W. Darnall, R.G. Wilkins (Eds), Vol. 2, Chap. 2, pp. 27–74, Elsevier, New York (1980).
[11] N. Komeda, H. Nagao, Y. Kushi, G. Adachi, M. Suzuki, A. Uehara, K. Tanaka. *Bull. Chem. Soc. Jpn*, **68**, 581 (1995).
[12] L. Casella, O. Carugo, M. Gullotti, S. Doldi, M. Frassoni. *Inorg. Chem.*, **35**, 1101 (1996).
[13] E. Monzani, G.J. Anthony, A. Koolhaas, A. Spandre, E. Leggieri, L. Casella, M. Gullotti, G. Nardin, L. Randaccio, M. Fontani, P. Zanello, J. Reedijk. *J. Biol. Inorg. Chem.*, **5**, 251 (2000).
[14] R.T. Stibrany, J.A. Potenza, H.J. Schugar. *Inorg. Chim. Acta*, **243**, 33 (1996).
[15] M. Scarpellini, A. Neves, E.E. Castellano, E.F. deAlmeida Neves, D.W. Franco. *Polyhedron*, **23**, 511 (2004).
[16] J.A. Halfen, S. Mahapatra, M.M. Olmstead, W.B. Tolman. *J. Am. Chem. Soc.*, **116**, 2173 (1994).
[17] J.A. Halfen, S. Mahapatra, E.C. Wilkinson, A.J. Gengenbach, V.G. Young, L. Que Jr, W.B. Tolman. *J. Am. Chem. Soc.*, **118**, 763 (1996).
[18] H. Yokoyama, K. Yamaguchi, M. Sugimoto, S. Suzuki. *Eur. J. Inorg. Chem.*, 1435 (2005).
[19] H. Nagao, N. Komeda, M. Mukaida, M. Suzuki, K. Tanaka. *Inorg. Chem.*, **35**, 6809 (1996).
[20] S. Nelson, J. Rodgers. *J. Chem. Soc. A*, 272 (1968).
[21] M. Shibata, M. Mori, E. Kyuno. *Inorg. Chem.*, **3**, 1573 (1964).
[22] A Computer Program for the Solution and Refinement of Crystal Structures for X-ray Diffraction Data, MAC Science Corporation, Yokohama, Japan (1994).
[23] M. Ciampolini, G.P. Speroni. *Inorg. Chem.*, **5**, 45 (1966).
[24] M. Ciampolini, N. Nardi, G.P. Speroni. *Coord. Chem. Rev.*, **1**, 222 (1966).
[25] F.A. Cotton, G. Wilkinson, C.A. Murillo, M. Bochmann. *Advanced Inorganic Chemistry*, 6th Edn, pp. 820–821, Wiley, New York (1999).
[26] E. Goldschmied, N.C. Stephenson. *Acta Cryst.*, **B26**, 1867 (1970).
[27] C.J. Davies, G.A. Solan, J. Fawcett. *Polyhedron*, **23**, 3105 (2004).
[28] M.I. Kay, B.C. Frazer. *Acta Cryst.*, **14**, 56 (1961).
[29] K. Nakamoto. *Infrared and Raman Spectra of Inorganic and Coordination Compounds*, 6th Edn. Part B, pp. 52–57, Wiley, New York (2009).
[30] M. Laing, S. Baines, P. Sommerville. *Inorg. Chem.*, **10**, 1057 (1971).
[31] B. Nuber, H. Siebert, K. Weidenhammer, J. Weiss, M.L. Ziegler. *Acta Cryst.*, **B35**, 1020 (1979).
[32] K.R. Maxcy, M.M. Turnbull. *Acta Cryst.*, **C55**, 1984 (1999).
[33] I. Bernal. *Inorg. Chim. Acta*, **96**, 99 (1985).
[34] I. Bernal, J. Cetrullo, J. Cai. *Transition Met. Chem.*, **19**, 221 (1994).